Supporting Information

Highly-efficient phenanthroline-based organic anode material with a three-electron redox mechanism

Kangkang Jia [a], Haitao Liu [a,c], Guimei Huang [a], Jingwei Zhang [a], Xiaorui Liu [d], Lu Li [b*], Linna Zhu [a,b*], Fei Wu [a,*]

[a] *Chongqing Key Laboratory for Advanced Materials and Technologies of Clean Energy, School of Materials & Energy, Southwest University, Chongqing 400715, P.R. China.*

[b] *Chongqing University Key Laboratory of Micro/Nano Materials Engineering and Technology, Chongqing University of Arts and Sciences, Yongchuan, Chongqing, 402160, P. R. China.*

[c] *Institute of Chemistry, Henan Academy of Sciences, Zhengzhou 450002, P. R. China.*

[d] *Key Laboratory of Luminescence Analysis and Molecular Sensing, Ministry of Education, School of Chemistry and Chemical Engineering, Southwest University, Chongqing 400715, P. R. China.*

Corresponding Author:

Linna Zhu, *School of Materials & Energy, Southwest University, Chongqing, China, E-mail address: lnzhu@swu.edu.cn. Tel.: +86 23 68254957.*

Fei Wu, *School of Materials & Energy, Southwest University, Chongqing, China, E-mail address: feiwu610@swu.edu.cn*

Contents

Table S1. Resistances of S-PD in Na-ion batteries obtained from equivalent circuit fitting of impedance data.

Table S2. Performance comparison of recently reported carboxylate electrode materials in sodium-ion batteries.

1.General Methods

Unless otherwise stated, all starting materials were purchased from commercial suppliers (Sigma Aldrich, and the Energy Chemical) and used without further purification. Potassium Fluoride (Adamas), N-Formylsaccharin (Adamas), Diethyl Carbonate (Acros), and 3,8-Dibromophenanthroline (Energy Chemical) were purchased and used without further purification.

2.Experimental Section

Materials Synthetic:

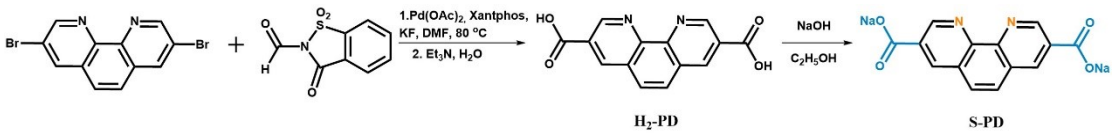

H_2-PD S-PD

Scheme S1 the synthetic route of compounds ***H_2-PD*** **and** ***S-PD*.**

Synthesis of 1,10-phenanthroline-3,8-dicarboxylic acid (H_2-PD):

In an argon-filled glovebox, Xantphos (0.3 mmol, 156.2 mg) and $Pd(OAc)_2$ (0.2 mmol, 40.3 mg) was added to a 50 mL heavy wall pressure vessel with a magnetic stir bar, followed by 25.0 mL of anhydrous N,N-dimethylformamide to dissolve the catalyst. Then 3,8-Dibromo-1,10-phenanthroline (2.9 mmol, 1.0 g), KF (15.0 mmol, 0.3 g) and N-formylsaccharin (7.5 mmol, 1.6 g) was added. The vessel was screw capped and heated with vigorous stirring at 80˚C in an oil bath for three days. After cooling to room temperature, 7 mL triethylamine and 10 mL water was added and the mixture was stirred at room temperature overnight. The solvent was removed under vacuum, the solid was suspended in water and filtered with copious amount of water. 1.0 g portions of the solid was heated and dissolved in 250.0 mL of 1 M NaOH aqueous solution and filtered through a cellulose membrane. The filtrate was acidified with 1 M HCl aqueous solution to about pH = 6 and the light orange precipitate was collected by filtration and washed with a large amount of water until the filtrate was neutral. The solid was rinsed with acetone and dried in vacuo to afford in total 648.1 mg of light orange product (81.7% yield). ^{1}H NMR (600 MHz, DMSO) δ 13.71 (s, 2H), 9.55 (s, 2H), 9.10 (s, 2H),

8.26 (s, 2H), ^{13}C NMR (151 MHz, DMSO) δ 166.62 (s), 150.34 (s), 147.44 (s), 138.61 (s), 129.15 (s), 128.43 (s), 126.47 (s). HR-MS (ESI): Calcd. for $[M-H]^-$: 267.0411, found: 267.0413.

Synthesis of Sodium 1,10-phenanthroline-3,8-dicarboxylate(S-PD):

To a stirred aqueous suspension (5.0 mL) of H_2-PD (0.5 g, 1.9 mmol), an aqueous solution (5.0 mL) of NaOH (0.2 g, 4.75 mmol) was added at room temperature. After the completion of the reaction, the solution was filtered, and ethanol (15.0 mL) was added to the filtrate, resulting in white precipitates. The white precipitate obtained was filtered, washed with ethanol, and dried in air. Yield: 524.1 mg (90.9%). ^{1}H NMR (600 MHz, D_2O) δ 9.20 (s, 2H), 8.48 (s, 2H), 7.59 (s, 2H). ^{13}C NMR (151 MHz, D_2O) δ 172.62 (s), 149.96 (s), 144.68 (s), 137.55 (s), 131.35 (s), 128.30 (s), 127.27 (s).

Material characterizations: The nuclear magnetic resonance (NMR) spectra were obtained from a BRUKER AVANCE III 600 MHz NMR Instrument (in $CDCl_3$). Data for ^{1}H NMR are recorded as follows: chemical shift (ppm), multiplicity (s, singlet; d, doublet; t, triplet; q, quarter; m, multiple), coupling constant (Hz), integration. Data for ^{13}C NMR are reported in terms of chemical shift (δ, ppm). JSM-7800F field emission scanning electron microscope was used to characterize morphology. The crystal structures were analyzed using MAXima-X XRD-7000. The Fourier transform infrared spectrometer (FT-IR) was recorded using KBr pellets on a Thermo Nicolet 6700 with the wavenumber range of 4000-400 cm^{-1}.

Electrochemical tests: For the half cell, the working electrodes were prepared by casting the slurry onto a clean Al foil, where the slurry contained the active materials

(70 wt%), carbon black (Super P, 20 wt%), and poly (vinylidene fluoride) binder (PVDF, 10 wt%). Then, the collector was dried overnight at 60 ^{o}C. The separator was Whatman glass fiber. The samples of electrochemically active materials were evaluated in 2032-type coin cells with a Na disk as the counter electrode and 1.0M $NaCF_3SO_3$ (in TETRAGLYME=100 Vol%, Duoduo chemical reagent Co., LTD, Suzhou). The average loading of active materials was 0.8~1.3 mg cm^{-2}. All battery assembly and disassembly are performed in a dry Ar-filled glove box (H_2O<0.1 ppm, O_2<0.1ppm Mikrouna).

The galvanostatic cycling test was carried on a CT-4008T instrument (Shen Zhen NEWARE electronic Co.). Cyclic voltammograms (CVs) were tested on a CHI instrument electrochemical workstation (Corrtest CS310H) at a scan rate of 0.1 mV s^{-1} between 0.1 and 2.6 V (vs Na^+/Na). The electrochemical impedance spectroscopy (EIS) test was measured by a CHI instrument electrochemical workstation in the frequency range of 10^{-2}-10^5 Hz at the amplitude of 5 mV. All the tests were performed at room temperature.

Ex-situ FTIR, ex-suit Raman, and ex-situ XPS spectroscopy: In an argon-filled glove box, the electrode sheets were taken out of the batteries at different charging and discharging states, and then washed with DME to remove the remaining electrolyte. It was then vacuum dried at 60°C for 6 hours. Then the marked electrodes were stored in an argon atmosphere. The samples were quickly taken out of the argon-filled box for each test. And these samples were exposed to air when conducting ex-situ measurements. For ex-situ FTIR tests, the products at different charge and discharge

states were tested using the ATR pattern. For ex-situ XPS tests, the sample was prepared in a stream of Ar-flow, and then the XPS measurement was conducted.

Computational details： Geometric structures and electronic properties of the investigated systems were fully optimized using B3LYP at 6-31G(d,p) levels.[1] The energies of all of the obtained geometries are ensured to be the lowest because the optimized structures do not exhibit imaginary frequency. All calculations were carried out by the Gaussian 09 program.[2]

XPS fitting method: The CasaXPS software was used to perform peak fitting of the original data, and the Origin2018 software was used to plot the exported data. In the process of fitting, the FWHM is limited to be between 1 and 2 eV.

GITT test:

The Na^+ diffusion coefficient (D_{Na^+}) was calculated by the galvanostatic intermittent titration technique measurement (GITT) method according to the following equation：

$$D_{Na^+} = \frac{4}{\pi}\left(\frac{n_m V_m}{S}\right)^2\left(\frac{\Delta E_s}{\tau\left(dE_t/d\sqrt{\tau}\right)}\right)^2 = \frac{4}{\pi\tau}\left(\frac{n_m V_m}{S}\right)^2\left(\frac{\Delta E_s}{\Delta E_t}\right)^2 \quad \text{.....（S1）}$$

where τ is the pulse time, n_m is the mole number, V_m is the molar volume, S is the electrode-electrolyte interface area, ΔE_S is the voltage difference between the steady-state and the initial state of every step, and ΔE_t is the change of total voltage during a pulse step excluding the *IR* drop. The molar volume of per sample repetitive unit was calculated by measuring the mass and the total volume of a pressed sample pellet (Figure S8), and the value was acceptable here when compared with some reported organic electrode materials. It is worth noting that the observed Na-ion diffusion

coefficient of organic materials is usually higher than that of inorganic electrodes composited by ionic bonds, because the solid/crystalline state of organic materials is mainly interacted by van der Waals forces, indicating that the organic material should be sodium ion transmission provides greater void space.

3.Spectra:

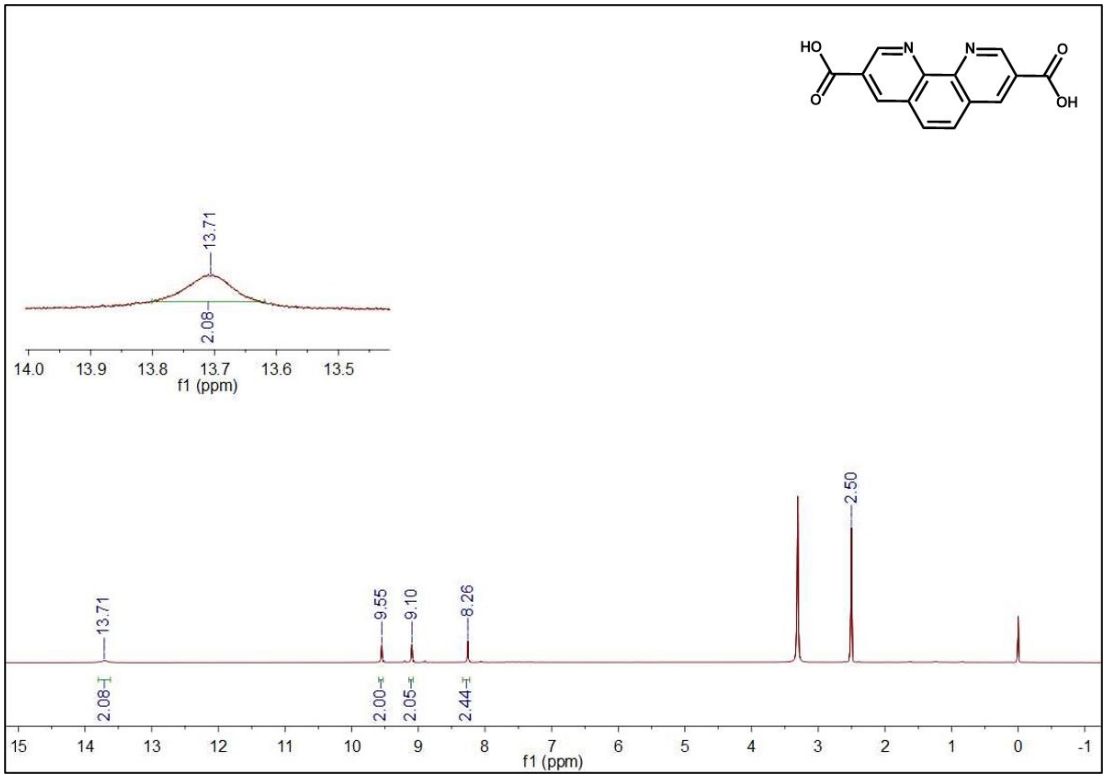

Figure S1. ^{1}H NMR spectrum of H_2-PD in DMSO.

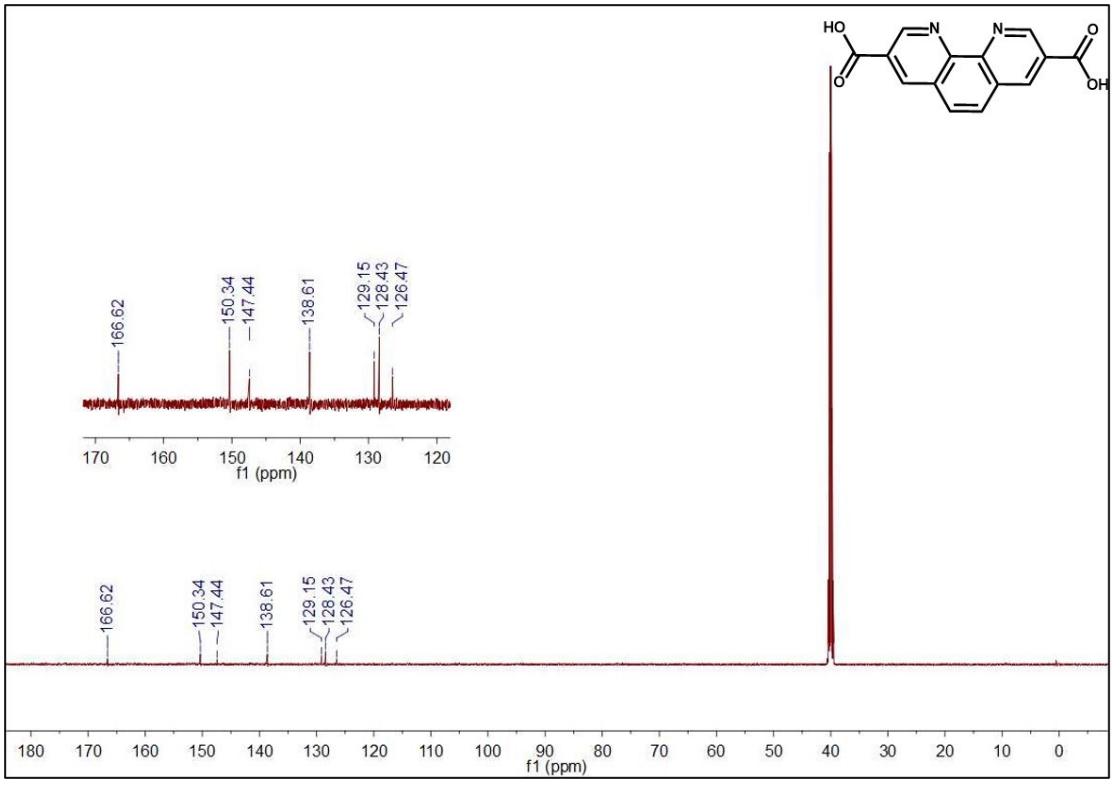

Figure S2. ^{13}C NMR spectrum of H_2-PD in DMSO.

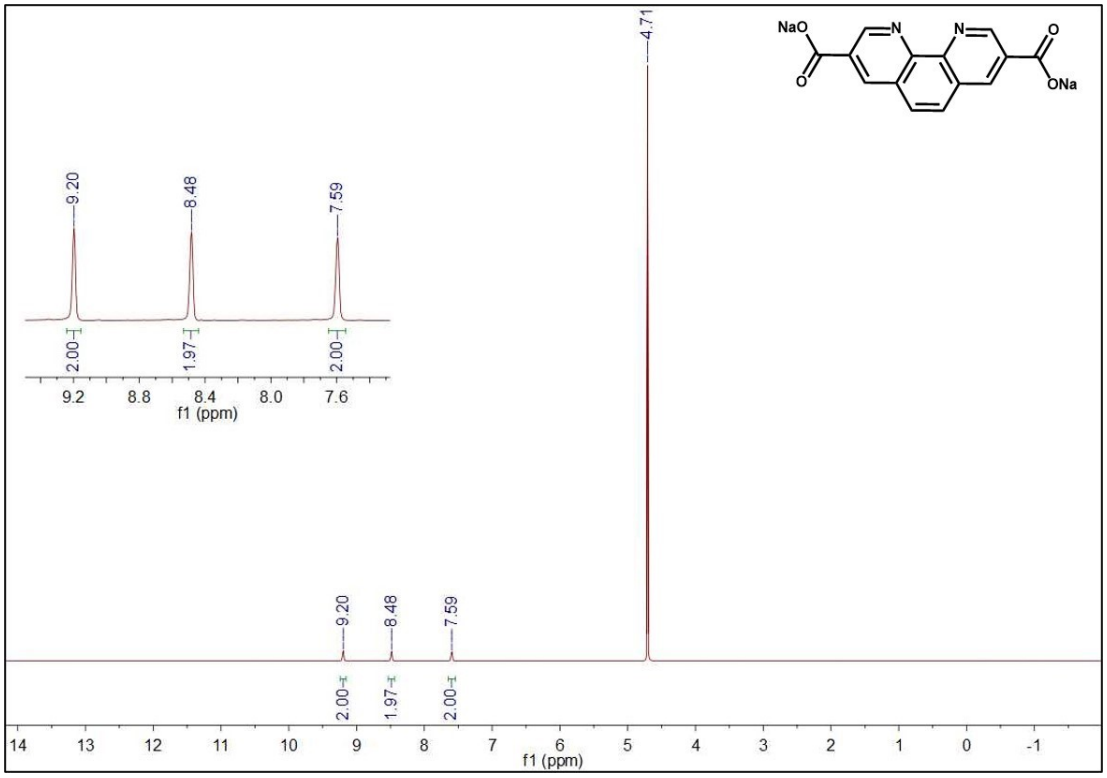

Figure S3. ^{1}H NMR spectrum of S-PD in D_2O.

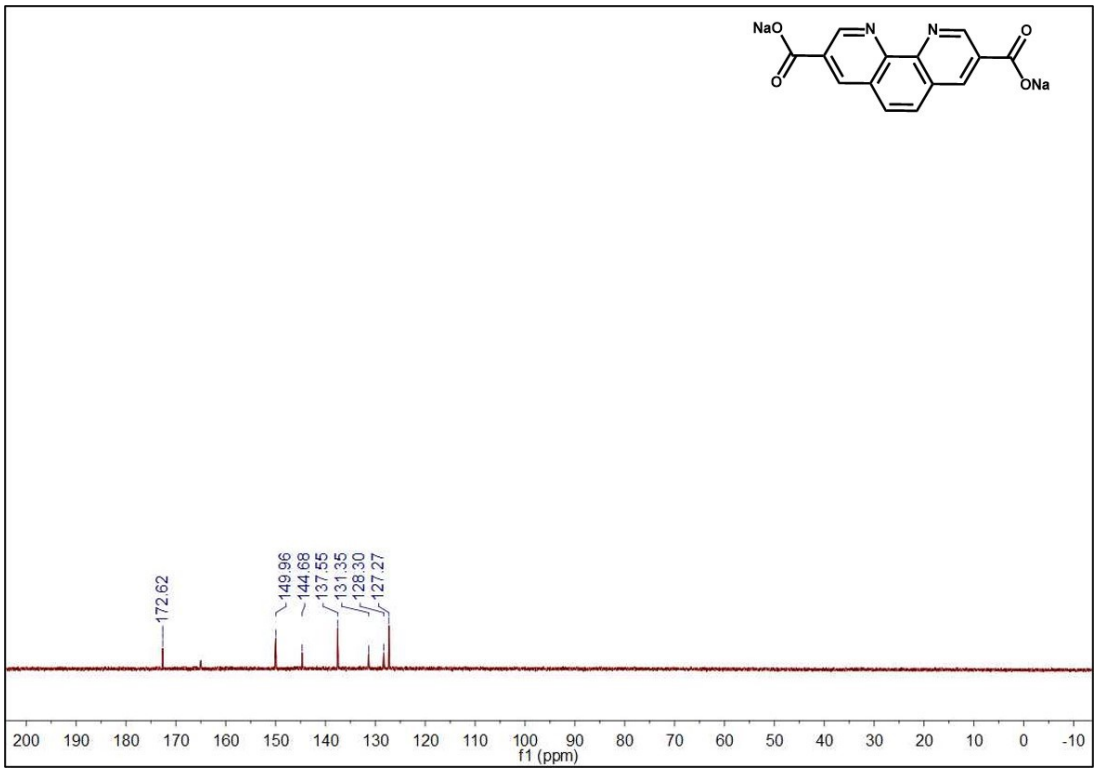

Figure S4. ^{13}C NMR spectrum of S-PD in D_2O.

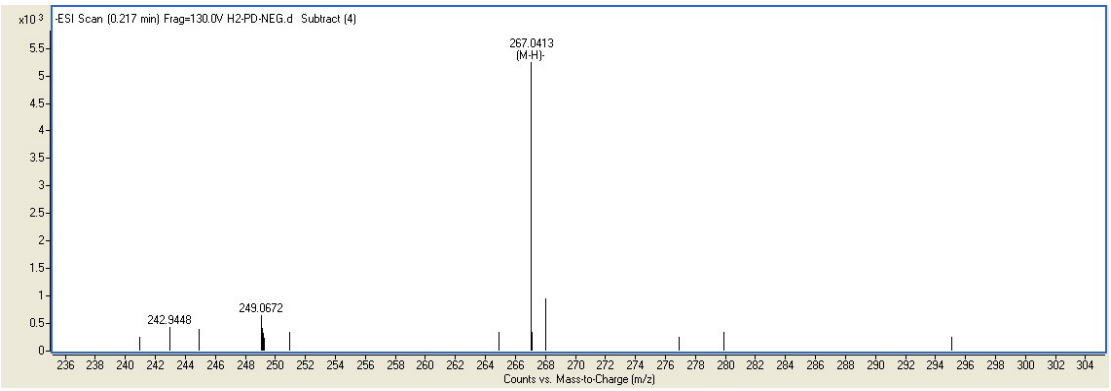

Figure S5. ESI-MS of H_2-PD.

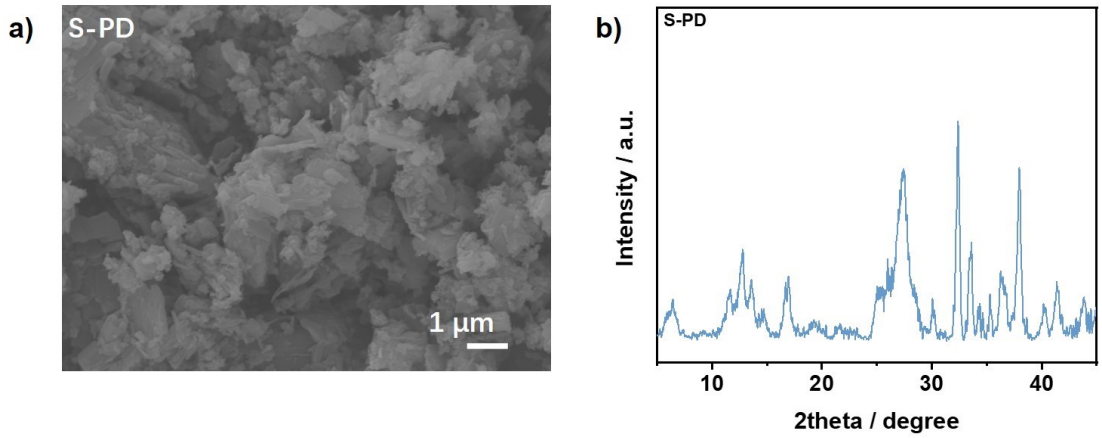

Figure S6. a) FESEM image and b) XRD spectra of S-PD.

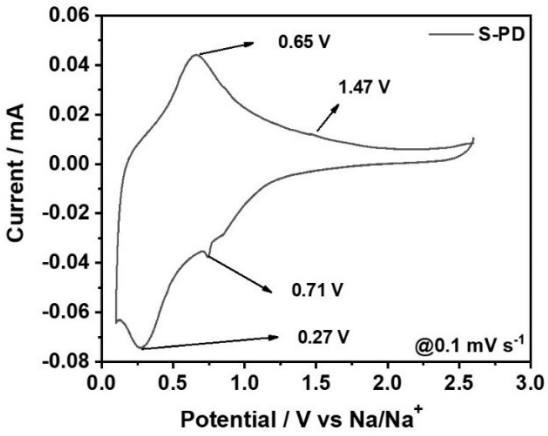

Figure S7. The CV curves of the S-PD anode.

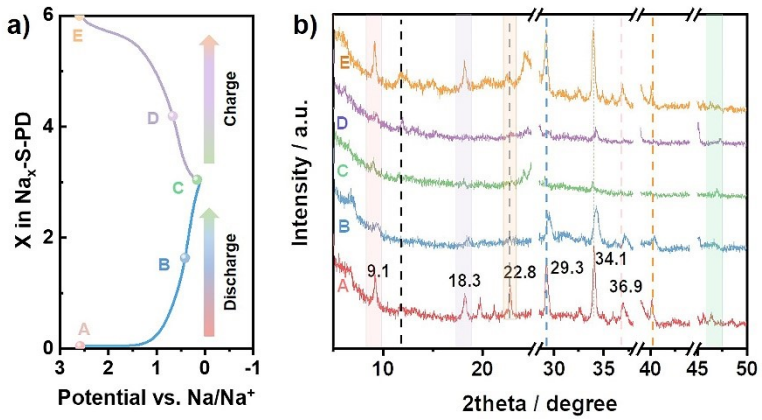

Figure S8. The second discharge/charge curves of S-PD electrode at 50 mA g^{-1} among the voltage range of 0.1-2.6 V and ex-situ studies were performed at different states as marked by A (pristine), B (0.4 V discharged), C (0.1 V discharged), D (0.6 V charged), and E (2.6 V charged), b) Ex-situ XRD spectra of S-PD.

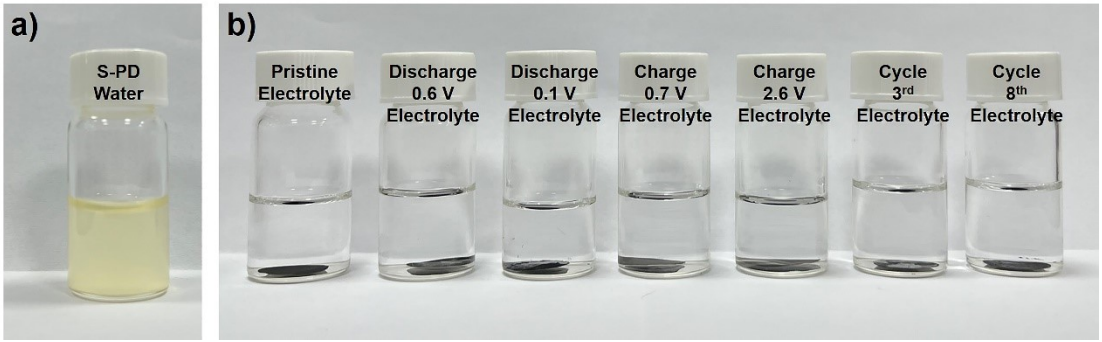

Figure S9. a) Photographs of the S-PD in water, b) Photographs of the S-PD electrodes in the electrolyte at different discharge/charge states after 7 days.

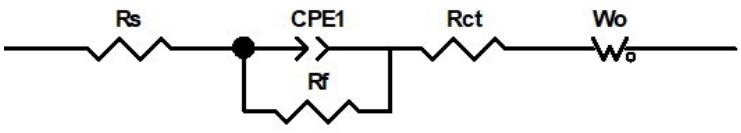

Figure S10. The equivalent circuits of EIS data for S-PD in Na-ion batteries.

R_s: electrolyte resistance, R_{ct}: charge transfer resistance, R_f: contact resistance of SEI films, CPE: constant phase element, and Wo: Warburg impedance. The simulated

impedance parameters were determined by fitting the original EIS spectra using ZView software (inset).

Figure S11. The S-PD pellet was obtained by the classic powder's pressing method (18 MPa).

The weight, thickness and diameter of the resulting pellet were 75.3 mg, 0.510 mm, and 13.077 mm, respectively. The molar volume (V_m) of the repeating unit of sample is about 283.9 cm^3 mol^{-1}.

Table S1. Resistances of S-PD in Na-ion batteries obtained from equivalent circuit fitting of impedance data.

Cycle	R_s (Ω)	R_f (Ω)	R_{ct} (Ω)
Pristine	4.18	3540	4599
5	8.564	301.9	160.5
30	7.167	314.2	127.2

Table S2. Performance comparison of recently reported carboxylate electrode materials in Na-ion batteries.

Anode	Electrode Composition	Capacity (mA h g^{-1}), current rate	Capacity Retention, Cycle	Reference
	70:20:10 X: Super P: PVDF	252 50 mA g^{-1}	83%, 100	This work
1	60:30:10 X: Super P: CMC	294 50 mA g^{-1}	90%, 90	[3]
1	64:16:10:10 X: KB: CB: PVDF	263 25.5 mA g^{-1}	74.4%, 50	[4]
2	5:3.5:1.5 X: Super P: PVDF	270 12.7 mA g^{-1}	83%, 100	[5]
3	65:30:5 X: Super P: PVDF	207 19 mA g^{-1}	89%, 100	[6]
4	60:33:7 X: CB: CMC	161.7 5.125 mA g^{-1}	47%, 40	[7]
5	60:30:10 X: acetylene black: CMC	115 25 mA g^{-1}	~100%, 100	[8]
6	57.1:28.6:14.3	200	~92%,	[9]

Anode	Electrode Composition	Capacity (mA h g^{-1}), current rate	Capacity Retention， Cycle	Reference
7	X: Super P: CMC 50:40:10 X: CB: CMC 6:3:1	20.3 mA g^{-1} 260 50 mA g^{-1}	150 90%, 50	[10]
8	X: CB: sodium alginate 54.6:15.4:20:10	170 0.2 C	100% , 100	[11]
9	X: CNT: Super P: sodium alginate 60: 30: 10	231 50 mA g^{-1}	80%, 100	[12]
10	X: Super P: sodium alginate 60: 30: 10	334 50 mA g^{-1}	96.5%, 200	[13]
11	X: acetylene black: sodium alginate 60: 30: 10	208 40 mA g^{-1}	70%, 100	[14]
12	X: CB: sodium alginate 60: 30: 10	192 20 mA g^{-1}	67%, 40	[15]
13	60: 30: 10	256	61%,	[16]

Anode	Electrode Composition	Capacity (mA h g^{-1}), current rate	Capacity Retention, Cycle	Reference
14	X: KB: PVDF 55:35:10 X: Super P：PVDF 60: 30: 10	25 mA g^{-1} 250 C/5	50 80%, 100	17
15	X: Super P: sodium alginate	426 50 mA g^{-1}	~100%, 50	18
16	70:20:10 X: Super P：PVDF	197 100 mA g^{-1}	99.1%, 350	19

Molecular structural formula：

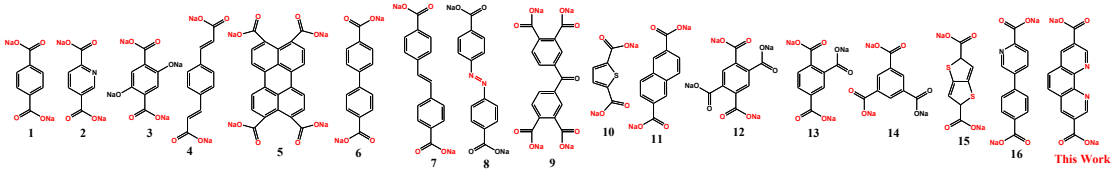

References:

1. A. Cohen, P. Mori-Sánchez and W. Yang, *Chem. Rev.*, 2012, **112**, 289-320.
2. M. J. Frisch, G. W. Trucks, H. B. Schlegel, G. E. Scuseria, M. A. Robb, J. R. Cheeseman, G. Scalmani, V. Barone and G. A. Petersson, *Fox, "Gaussian 09," Revision A.1, Gaussian, Inc., Wallingford, 2009.*
3. Y. Park, D. S. Shin, S. H. Woo, N. S. Choi, K. H. Shin, S. M. Oh, K. T. Lee and S. Y. Hong, *Adv. Mater.*, 2012, **24**, 3562-3567.
4. L. Zhao, J. Zhao, Y.-S. Hu, H. Li, Z. Zhou, M. Armand and L. Chen, *Adv. Energy. Mater.*, 2012, **2**, 962-965.
5. H. Padhy, Y. Chen, J. Lüder, S. R. Gajella, S. Manzhos and P. Balaya, *Adv. Energy. Mater.*, 2018, **8**, 1701572.
6. S. Wang, L. Wang, Z. Zhu, Z. Hu, Q. Zhao and J. Chen, *Angew. Chem. Int. Ed. Engl.*, 2014, **53**, 5892-5896.
7. V. A. Mihali, S. Renault, L. Nyholm and D. Brandell, *RSC Adv.*, 2014, **4**, 38004-38011.
8. R. R. Zhao, Y. L. Cao, X. P. Ai and H. X. Yang, *J. Electroanal. Chem.*, 2013, **688**, 93-97.
9. A. Choi, Y. K. Kim, T. K. Kim, M.-S. Kwon, K. T. Lee and H. R. Moon, *J. Mater. Chem. A*, 2014, **2**, 14986-14993.
10. C. Wang, Y. Xu, Y. Fang, M. Zhou, L. Liang, S. Singh, H. Zhao, A. Schober and Y. Lei, *J. Am. Chem. Soc.*, 2015, **137**, 3124-3130.
11. C. Luo, G. L. Xu, X. Ji, S. Hou, L. Chen, F. Wang, J. Jiang, Z. Chen, Y. Ren, K. Amine and C. Wang, *Angew. Chem. Int. Ed. Engl.*, 2018, **57**, 2879-2883.
12. L. Y. Wang, C. Ma, X. Wei, B. B. Chang, K. X. Wang and J. S. Chen, *J. Mater. Chem. A*, 2020, **8**, 8469-8475.
13. C. Ma, L. Wu, Z. Jin, X. Y. Zhao, Y. S. Liu, Y. L. Bai, H. Sun, K. X. Wang and J. S. Chen, *Chem. Mater.*, 2018, **30**, 8426-8430.
14. V. Medabalmi, N. Kuanr and K. Ramanujam, *J. Electrochem. Soc.*, 2018, **165**, A175-A180.
15. K. Qin, K. Holguin, M. Mohammadiroudbari and C. Luo, *Chem. Commun. (Camb)*, 2021, **57**, 2360-2363.
16. T. Gu, S. Gao, J. Wang, S. Cao, K. Wang, M. Zhou and K. Jiang, *Chemelectrochem*, 2020, **7**, 3517-3521.
17. A. Tripathi, Y. Chen, H. Padhy, S. Manzhos and P. Balaya, *Energy Technology*, 2019, **7**, 1801030.
18. C. Ma, L.-Y. Wang, M.-H. Shu, C.-C. Hou, K.-X. Wang and J.-S. Chen, *J. Mater. Chem. A*, 2021, **9**, 11530-11536.
19. K. Jia, L. Zhu and F. Wu, *ChemSusChem*, 2021, **14**, 3124-3130.